Pathology - Research and Practice 215 (2019) 68–81

Contents lists available at ScienceDirect

Pathology - Research and Practice

journal homepage: www.elsevier.com/locate/prp

Microarray-based measurement of microRNA-449c-5p levels in hepatocellular carcinoma and bioinformatic analysis of potential signaling pathways

Li Jiang[a], Chang-Liang Wu[b], Ji-Zhou Wu[a], Xia Yang[c], Han-lin Wang[c], Guo-Jian Li[a,*]

[a] Department of Infectious Disease, The First Affiliated Hospital of Guangxi Medical University, Nanning, Guangxi Zhuang Autonomous Region, China
[b] Department of Gastroenterology, The Second Affiliated Hospital of Guangxi Medical University, Nanning, Guangxi Zhuang Autonomous Region, China
[c] Department of Pathology, The First Affiliated Hospital of Guangxi Medical University, Nanning, Guangxi Zhuang Autonomous Region, China

ARTICLE INFO

Keywords:
MicroRNA microarray
miR-449c-5p
Hepatocellular carcinoma
Pathways
Bioinformatics

ABSTRACT

The clinical role and potential molecular mechanisms of microRNA-449c-5p (miR-449c-5p) in hepatocellular carcinoma (HCC) tissues remains unclear. Combining multiple bioinformatic tools, we studied the miR-449c-5p expression levels in HCC tissues and explored possible target genes and related signaling pathways. First, miR-449c-5p expression data from microarrays provided by publicly available sources were mined and analyzed using various meta-analysis methods. Next, genes that were downregulated after miR-449c-5p mimic transfection into HCC cells were identified, and in silico methods were used to predict potential target genes. Several bioinformatic assessments were also performed to evaluate the possible signaling pathways of miR-449c-5p in HCC. Five microarrays were included in the current study, including GSE98269, GSE64632, GSE74618, GSE40744 and GSE57555. The standard mean difference was 0.44 (0.07–0.80), and the area under the curve was 0.68 (0.63–0.72), as assessed by meta-analyses, which consistently indicated the upregulation of miR-449c-5p in HCC tissues. A total of 2244 genes were downregulated after miR-449c-5p mimic transfection into an HCC cell line, while 5217 target genes were predicted by in silico methods. The overlap of these two gene pools led to a final group of 428 potential target genes of miR-449c-5p. These 428 potential target genes were primarily enriched in the homologous recombination pathway, which includes *DNA Polymerase Delta 3* (*POLD3*). Data mining with Oncomine and the Human Protein Atlas showed a decreasing trend in POLD3 mRNA and protein levels in HCC tissue samples. This evidence suggests that miR-449c-5p could play an essential role in HCC through various pathways and that *POLD3* could be a potential miR-449c-5p target. However, these in silico findings should be validated with further experiments.

1. Introduction

Hepatocellular carcinoma (HCC) is a subtype of primary liver cancer that has a poor prognosis. HCC pathogenesis is complex, and several molecular events play key roles in HCC development [1–5]. Many microRNAs (miRNAs) have been shown to regulate the expression of cancer-related genes in HCC [6–8]. However, the clinical significance and molecular mechanisms of some HCC-related miRNAs remains unknown.

Among the known miRNAs, microRNA-449c-5p (miR-449c-5p, accession number: MIMAT0010251, previous name: miR-449c) has not been widely studied. In non-cancer diseases, miR-449c-5p has been reported to have a suppressive effect on the osteogenic differentiation of valve interstitial cells. Thus, miR-449c-5p may be a prospective target for treating calcific aortic valve disease (CAVD) [9]. In cancers, the function and targets of miR-449c-5p have been studied in several types of neoplasia. miR-449c-5p levels have been shown to be remarkably reduced in the malignant cells and clinical cases of osteosarcoma [10], non-small cell lung cancer (11), nasopharyngeal carcinoma (12) and gastric carcinoma [13,14]. The expression levels and clinical implications of miR-449c-5p in HCC have not been previously reported. Several miR-449c-5p target genes have been confirmed in different diseases, including *6-phosphofructo-2-kinase* [14], *MET* [13], *c-MYC* [10,11] and *SMAD4* [9]. Since miRNA exerts its biological function through complementary combination with a target, many miR-449c-5p target genes may still be unknown. To date, the function of the

* Corresponding author at: Department of Infectious Disease, No.6 Shuangyong Road, Qingxiu District, The First Affiliated Hospital of Guangxi Medical University, Nanning, Guangxi Zhuang Autonomous Region, 530021, China.
E-mail address: liguojianaaa@163.com (G.-J. Li).

https://doi.org/10.1016/j.prp.2018.10.007
Received 11 August 2018; Received in revised form 15 September 2018; Accepted 17 October 2018
0344-0338/ © 2018 Elsevier GmbH. All rights reserved.

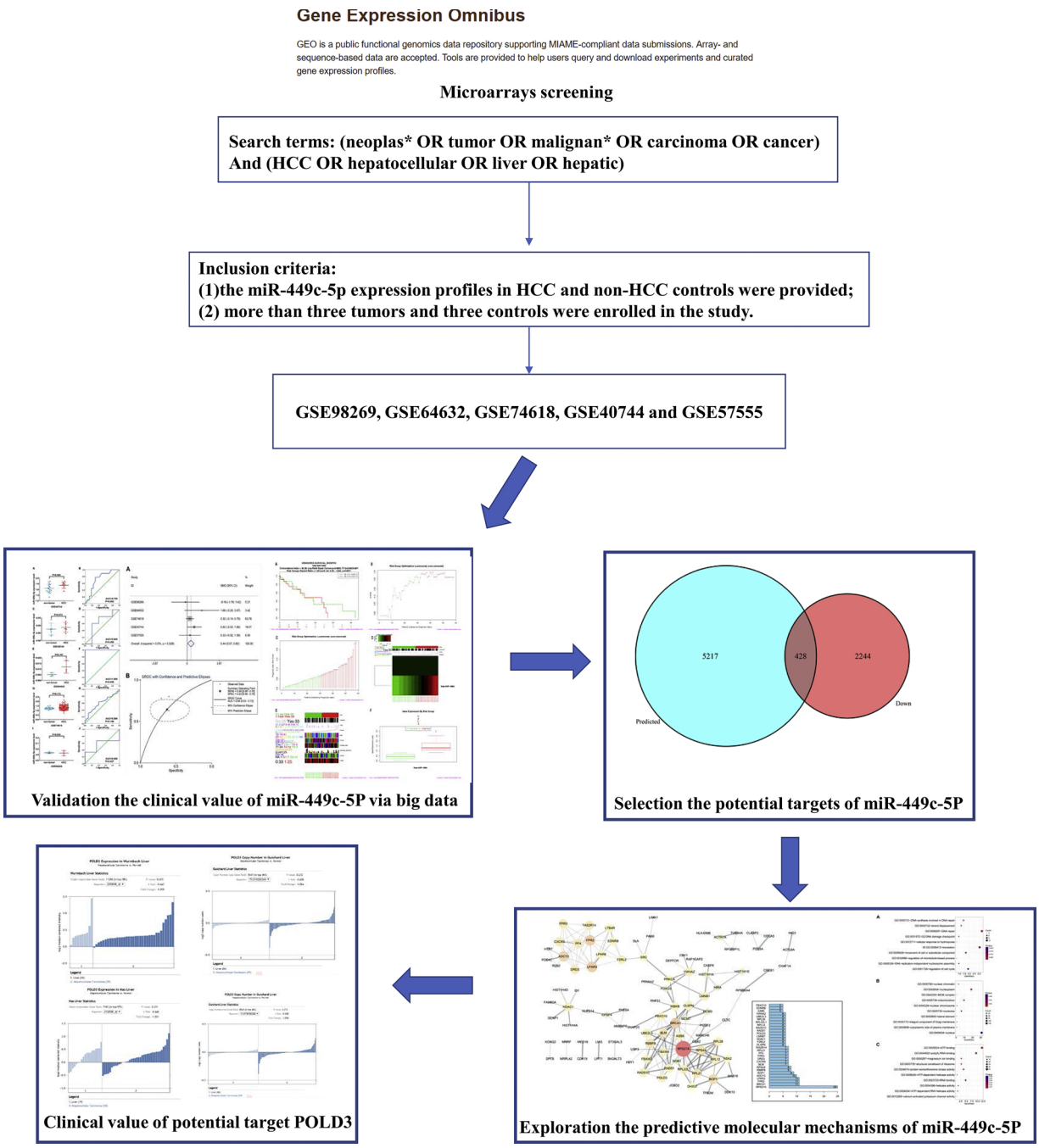

Fig. 1. Flow chart of the present study.

Table 1
The microarrays included in the current study.

GEO series	First author	Year	Country	Test platform	Number of included samples
GSE40744	Diaz G	2013	USA	Affymetrix	26
GSE57555	Murakami Y	2015	Japan	Agilent	10
GSE64632	Peng H	2015	USA	Exiqon	6
GSE74618	Martinez-Quetglas I	2016	Spain	Affymetrix	238
GSE98269	Xie Z	2017	China	Agilent	6

miR-449 family (including miR-449a, miR-449b and miR-449c) in HCC has only been investigated by one group [15], who used in vitro and in vivo experiments. That study verified that *SRY-box 4 (*SOX4*)* could be directly targeted by the miR-449 family, but the study focused on the miR-449 family as a whole part. The clinical role of miR-449c-5p in HCC and the possibility of additional target genes are both worthy of investigation.

Accordingly, we studied the role of miR-449c-5p in the clinical tissues of HCC patients, as well as the potential molecular mechanisms of this miRNA. First, we mined miR-449c-5p expression data from microarrays provided by publicly available sources. Next, genes that were downregulated after miR-449c-5p mimic transfection into HCC cells were identified, and in silico methods were used to predict potential target genes. Multiple bioinformatic assessments were performed to evaluate possible miR-449c-5p signaling pathways in HCC. Finally, the relationships between several potential target genes and miR-449c-5p were examined (Fig. 1).

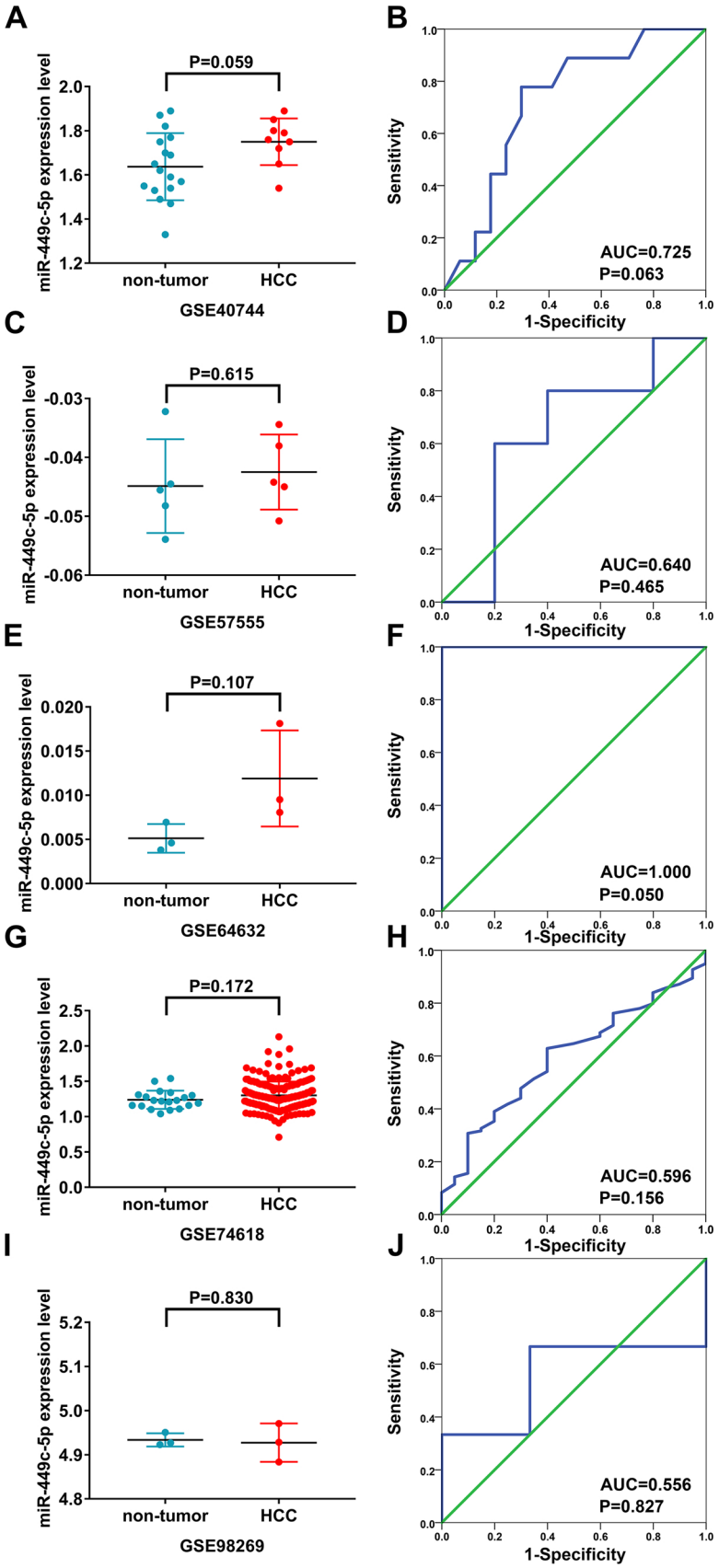

Fig. 2. miR-449c-5p expression levels in the microarray data in hepatocellular carcinoma (HCC). Scatter plots (A, C, E, G and I) and receiver operating characteristic (ROC) curves (B, D, F, H and J) were used to show the miR-449c-5p expression levels in the hepatocellular carcinoma (HCC) samples. AUC = area under the curve.

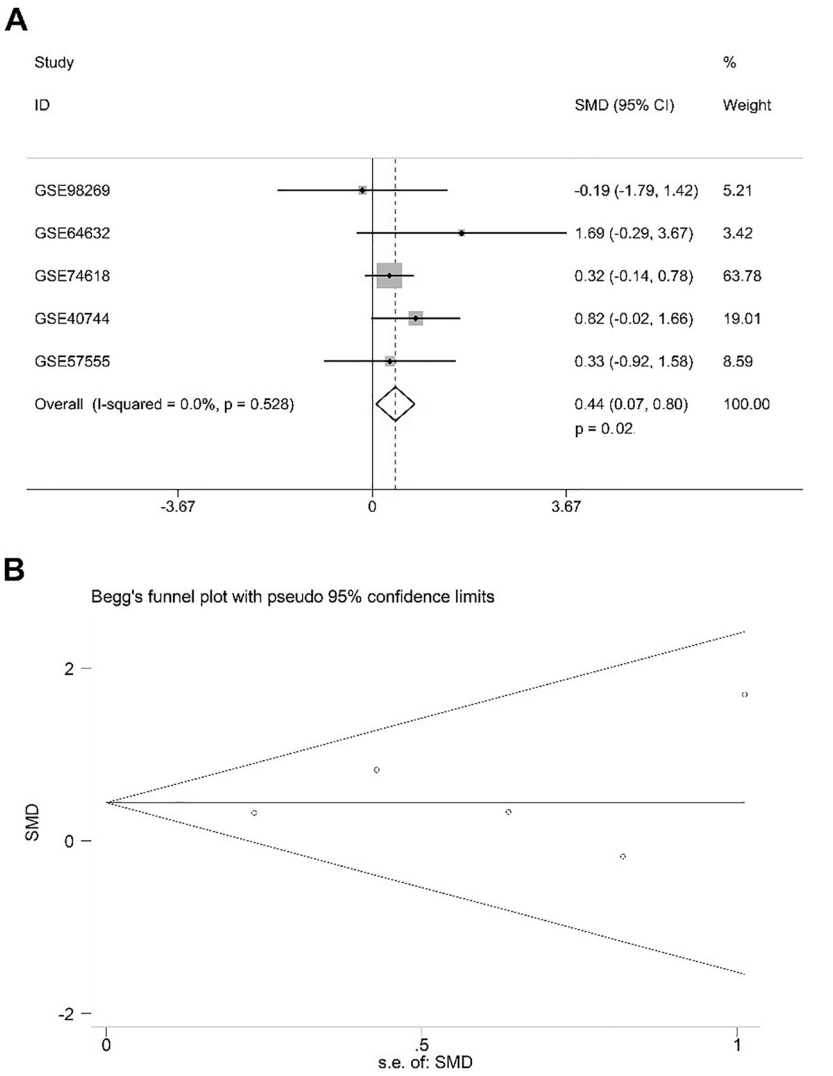

Fig. 3. Meta-analyses of miR-449c-5p expression levels in the hepatocellular carcinoma (HCC) samples. A: The Forest plot of standard mean difference (SMD) indicates that miR-449c-5p was significantly regulated in the HCC samples compared to non-tumor tissues; B: The Egger's funnel plot indicates that there was no publication bias. CI = confidence interval.

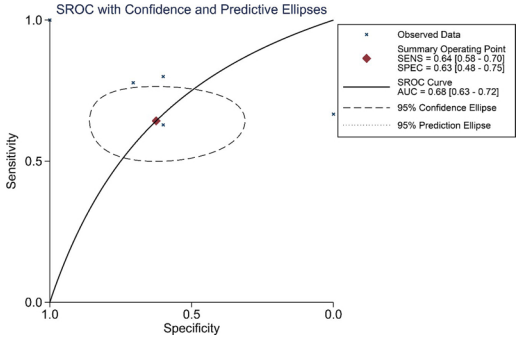

Fig. 4. The summary receiver operating characteristic curve (sROC) shows that miR-449c-5p expression levels can distinguish hepatocellular carcinoma (HCC) from non-tumor tissues.

2. Materials and Methods

2.1. Clinical role of miR-449c-5p in HCC tissues

2.1.1. Selection of relevant microarray and miRNA sequence data

To comprehensively assess the expression levels of miR-449c-5p (sequence: uaggcaguguauugcuagcggcugu) in HCC and corresponding non-tumor tissues, we collected miRNA microarrays and miRNA sequence data from Gene Expression Omnibus (GEO), Oncomine and ArrayExpress [16–21]. The following search terms were used: (neoplas* OR tumor OR malignan* OR carcinoma OR cancer) AND (HCC OR hepatocellular OR liver OR hepatic). A study was included if (1) the miR-449c-5p expression profiles in HCC and non-HCC controls were provided and (2) more than three tumors and three controls were enrolled in the study. The screening procedure was performed by three authors (Li Jiang, Xia Yang and Han-lin Wang).

2.1.2. Assessment of the miR-449c-5p expression levels

The miR-449c-5p expression level data were extracted from the included datasets, which contained three Agilent and two Affymetrix chips. Hybridization signals of miRNAs were standardized following the protocol of microarray. Standardized data stored in the matrix file was used to identify the expression profiles of miR-449c-5p in a single data set. Data were presented in the form of mean ± SD for further integration. Differences in the miR-449c-5p expression levels between HCC and non-HCC cells were analyzed using the Student's *t*-test with the SPSS software version 22.0. The ability of miR-449c-5p to distinguish HCC tissues from non-tumor tissues in each microarray was also calculated using the area under the curve (AUC) in receiver operating

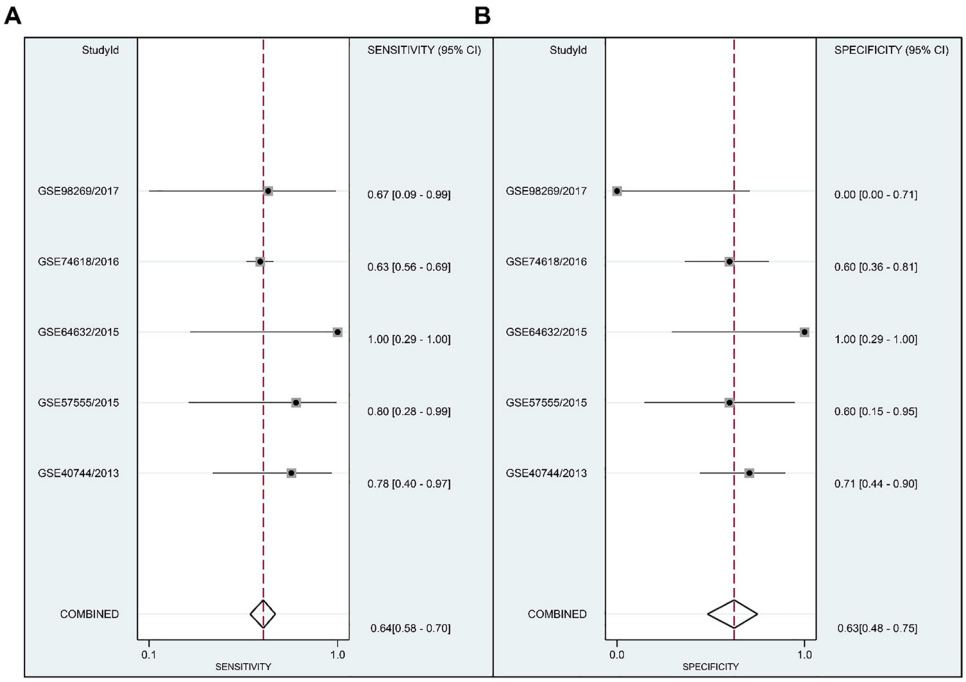

Fig. 5. Forest plots of sensitivity (A) and specificity (B) analyses for the studied microarrays.

characteristic (ROC) analysis. To obtain an overview of the clinical role of miR-449c-5p in HCC, a meta-analysis was performed using the Stata software version 14.0. The pooled data was assessed using the standard mean difference (SMD) and a 95% confidence interval (CI). A random or fixed model was selected according to the heterogeneity of the data. When the heterogeneity among the microarrays reached $I^2 > 50\%$ or $P < 0.05$, a random effects model was performed. Otherwise, a fixed effects model was preferred. To obtain more credible results, the Begg's and Egger's tests were conducted to detect publication bias [22–24]. In addition, a summary receiver operating characteristic (sROC) curve was generated, and the corresponding AUC was used to assess the ability of miR-449c-5p to distinguish HCC tissues from non-tumor samples. Sensitivity and specificity were also calculated using the Stata software to assess the ability of miR-449C-5p to distinguish HCC tissues from non-cancerous liver tissues [25–27]. The SurvMicro software (which assesses prognostic miRNA signatures) was used to examine the prognostic values of miR-449c-5p in HCC cohorts based on the Cox survival analysis [28,29].

2.2. Potential molecular mechanisms of miR-449c-5p in HCC

2.2.1. Identification of genes that were directly influenced by miR-449c-5p

To explore the regulatory mechanisms of miR-449c-5p, the databases were searched for differentially expressed genes (DEGs) post miR-449c-5p mimic or inhibitor transfection into HCC cells. GEO and ArrayExpress profiles were screened with the keywords mentioned above, and the corresponding datasets were downloaded. The fold change (FC) expression differences between the experimental groups that interfered with the miR-449c-5p mimics or inhibitors and the negative control groups were calculated using the Limma package of R software. Genes with FC values less than 0.5 or more than 2 and with P values less than 0.05 were regarded as DEGs for the current study.

2.2.2. Predicted miR-449c-5p targets

Predicted miR-449c-5p target genes were then obtained using the miRWalk software version 3.0 [30–32]. The score used to predict the targets of miR-449c-5p was calculated by using TarPmiR algorithm for miRNA target site prediction. The score represents the probability of interactions between miRNAs and mRNAs. Target genes with a combined score of 1 were selected, as these had the highest possibility of being actual miR-449c-5p targets. To further increase the reliability of the selected target genes, in silico methods were used to overlap the predicted target genes with the DEGs that were directly influenced by miR-449c-5p.

2.2.3. Relevant miR-449c-5p signaling pathways

The overlapping genes identified in the above steps were subjected to various bioinformatic analyses. The Database for Annotation, Visualization and Integrated Discovery (DAVID) analysis was used to perform gene functional enrichment analyses that included the Kyoto Encyclopedia of Genes and Genomes (KEGG) and the Gene Ontology (GO) database. The latter analysis was further divided into distinct annotation groups: biological process (BP), cell components (CC), and molecular function (MF) [33,34]. The results were visually displayed using the ggplot2 package of R software. The STRING database was used to analyze the protein-protein interactions (PPI) of the target genes. A combined score > 0.9 was set as the cut-off value to define the hub genes. A PPI network was constructed using the Cytoscape software. The hub genes in the network were calculated based on the number of connected nodes [35,36]. Finally, the mRNA levels of an example target gene were displayed using the Oncomine database [37–39], and the protein levels were displayed using the Protein Atlas database [40–43].

3. Results

3.1. Clinical role of miR-449c-5p in HCC tissues

3.1.1. Microarray data related to miR-449c-5p expression levels

According to the inclusion and exclusion criteria, five microarrays were included in the current study, including GSE98269, GSE64632, GSE74618, GSE40744 and GSE57555 (Table 1). The literature was also searched for miR-449c-5p expression data, but no literature reports were identified that could be used in the current study.

3.1.2. miR-449c-5p expression levels in HCC tissues

Among the five studied microarrays, the miR-449c-5p expression levels showed increasing trends, except in GSE98269 (Fig. 2). To

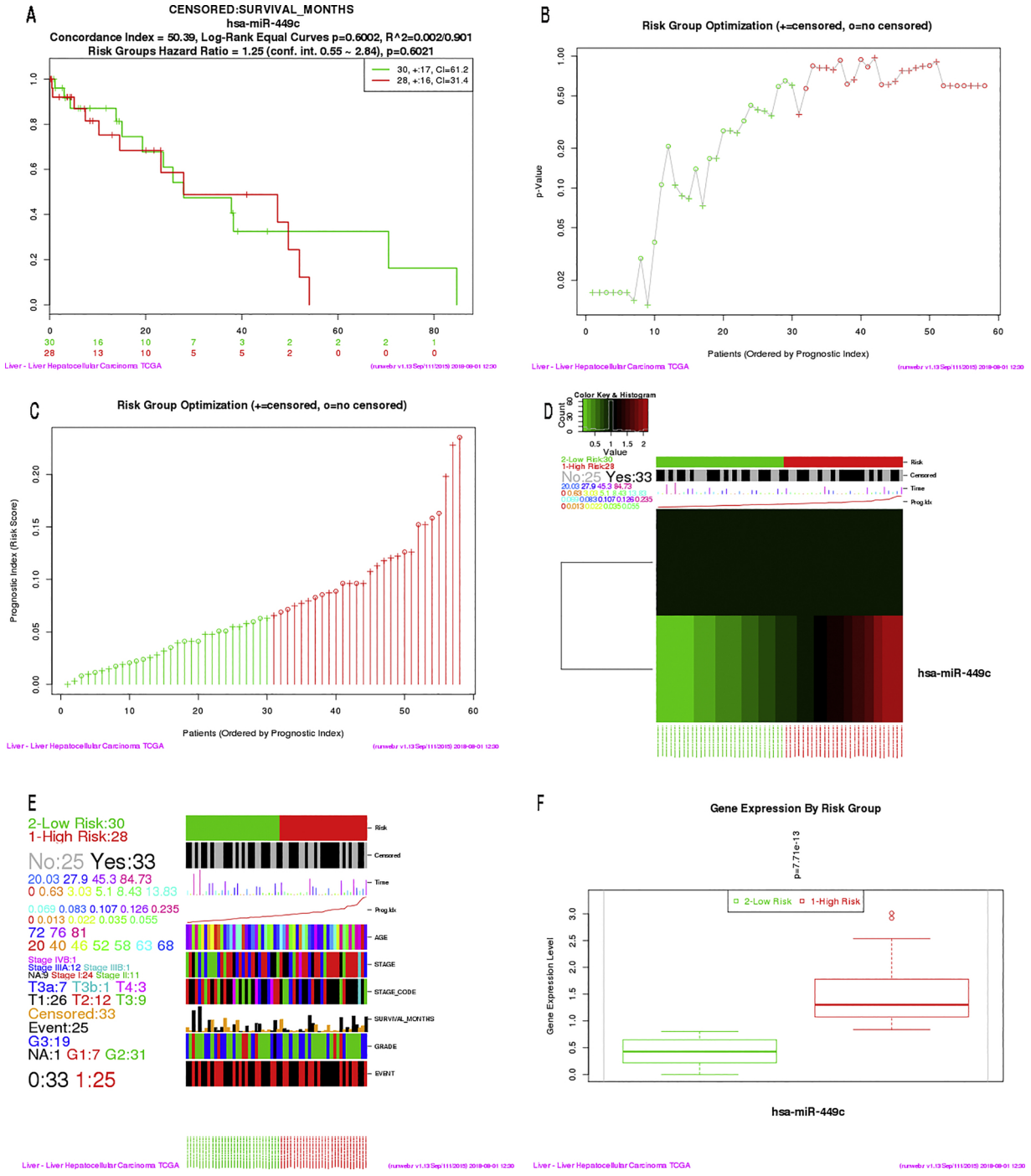

Fig. 6. The prognostic ability of miR-449c-5p expression levels in hepatocellular carcinoma (HCC), based on the The Cancer Genome Atlas (TCGA) data. A: Kaplan-Meier (K–M) curve; B: Curve of risk group optimization; C: Bars of risk group optimization; D: Heat map of the prognostic index of the miR-449c-5p expression levels; E: Heat map of the prognostic index of the miR-449c-5p expression levels and other clinicopathological parameters; F: miR-449c-5p expression by risk group.

provide an overview of the differences in the miR-449c-5p expression levels between the HCC and non-HCC samples, the SMD was calculated and found to be 0.44 (0.07–0.80, P = 0.02) (Fig. 3A). This SMD value reflected that miR-449c-5p expression levels were upregulated in HCC tissues (based on 238 HCC samples and 48 non-tumor samples). The Egger's test indicated that there was no statistically significant publication bias (Fig. 3B). These findings were also observed using another statistical approach. The individual AUCs of the miR-449c-5p expression levels were all higher than 0.55 in the ROC analysis (Fig. 2). Interestingly, the sROC analysis revealed that an AUC of 0.68 (0.63–0.72) could be reached when the data from the five microarrays were combined (Fig. 4). This again suggested that miR-449c-5p expression could distinguish HCC tissues from non-HCC tissues with a sensitivity of 0.64 and a specificity of 0.63 (Fig. 5).

Four sets of microarray/miRNA sequence data were available in the SurvMicro database: Li Gu Liver GSE10694, Wei Wang Liver GSE31384, Liver Hepatocellular Carcinoma TCGA and Budhu Wei_Wang Liver GSE6857. Among these, only the TCGA data provided the patient survival information relative to the miR-449c-5p expression (Fig. 6). When the HCC cases were divided into high-risk and low-risk groups based on

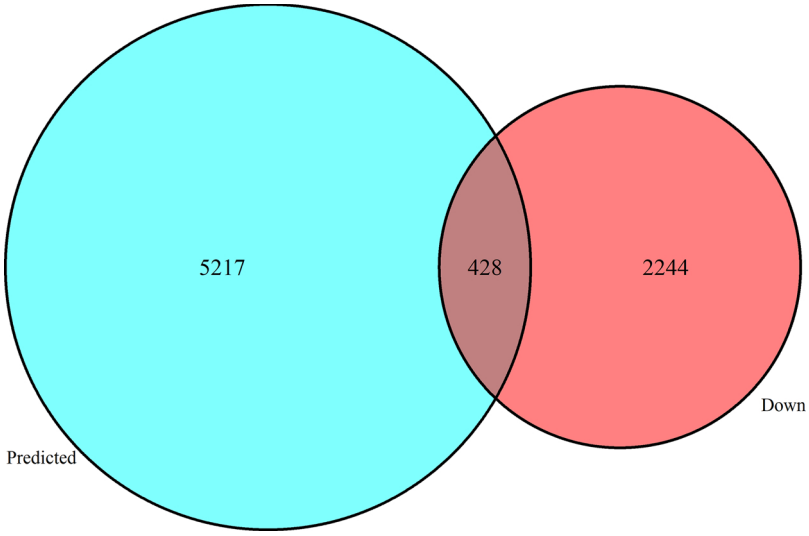

Fig. 7. The overlapping miR-449c-5p target genes in the hepatocellular carcinoma (HCC) samples. The integration of the 5217 predicted genes with the 2244 downregulated genes after miR-449c-5p transfection led to a final set of 428 target genes.

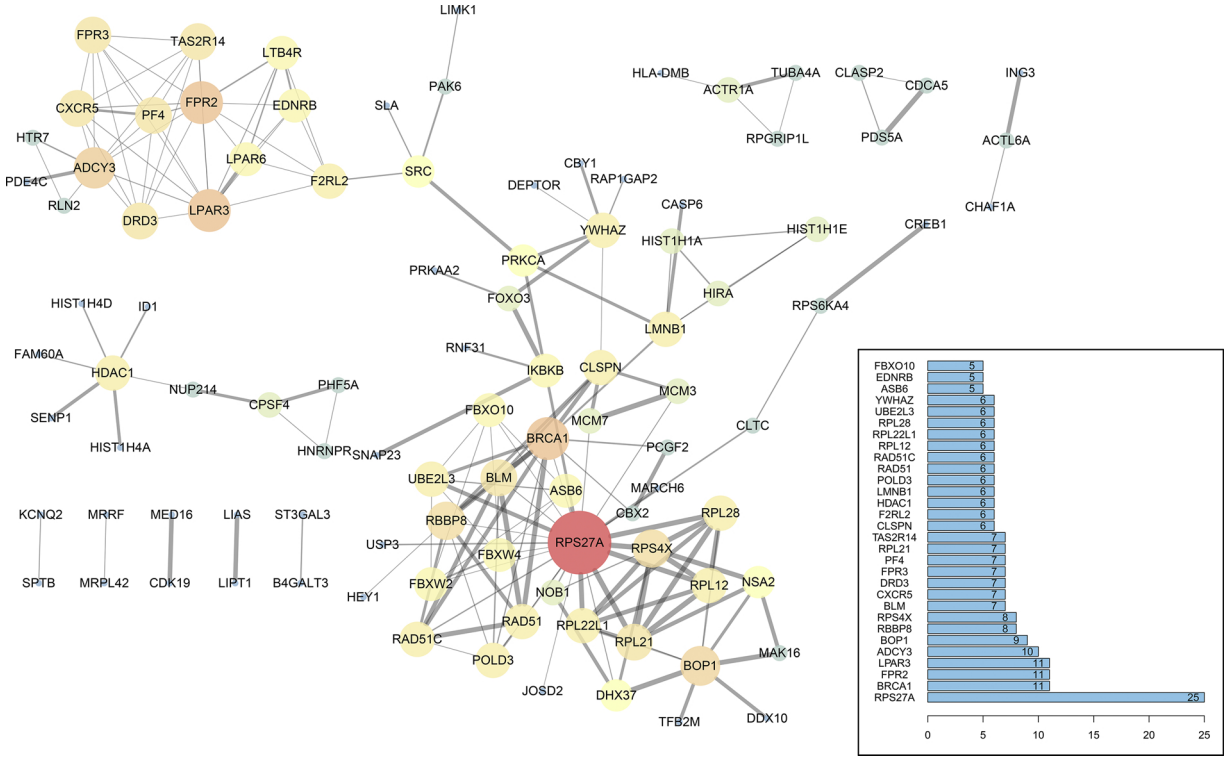

Fig. 8. A protein-protein interaction (PPI) network of the potential miR-449c-5p targets in the hepatocellular carcinoma (HCC) tissue samples. The String program was used to construct the PPI network. The PPI network displayed the interacting relationships among these genes. A greater size indicates a greater weight.

the cut-off expression level value of miR-449c-5p determined statistically, no significant survival difference was found between the high-risk and low-risk groups, with a hazard ratio (HR) of 1.25 (0.55–2.84).

3.2. Potential molecular mechanisms of miR-449c-5p in HCC

3.2.1. DEGs directly influenced by miR-449c-5p

According to the study's inclusion and exclusion criteria, only one microarray dataset with the interreference of miR-449c-5p in HCC cells was identified (GSE74710 [15]). In the GSE74710 study, the HCC cell line HLE was treated with 50 nM control doses of Allstars negative control (GSM1930719, HLE_NC_1 and GSM1930720, HLE_NC_2). The experimental groups were transfected with miScript miR-449c-5p mimics (GSM1930725, HLE_449c_1 and GSM1930726, HLE_449c_2). The GPL17077 platform from the Agilent-039494 SurePrint G3 Human GE v2 8 x 60 K Microarray 039381 (probe name version) was used to profile the DEGs. Since miR-449c-5p was overexpressed in the transfected cells, the downregulated genes (n = 2244) were collected for further analysis.

3.2.2. Potential miR-449c-5p target genes

Meanwhile, 5217 potential miR-449c-5p target genes were predicted using the online database miRWalk. The overlap of these potential target genes with the 2244 directly influence genes led to the

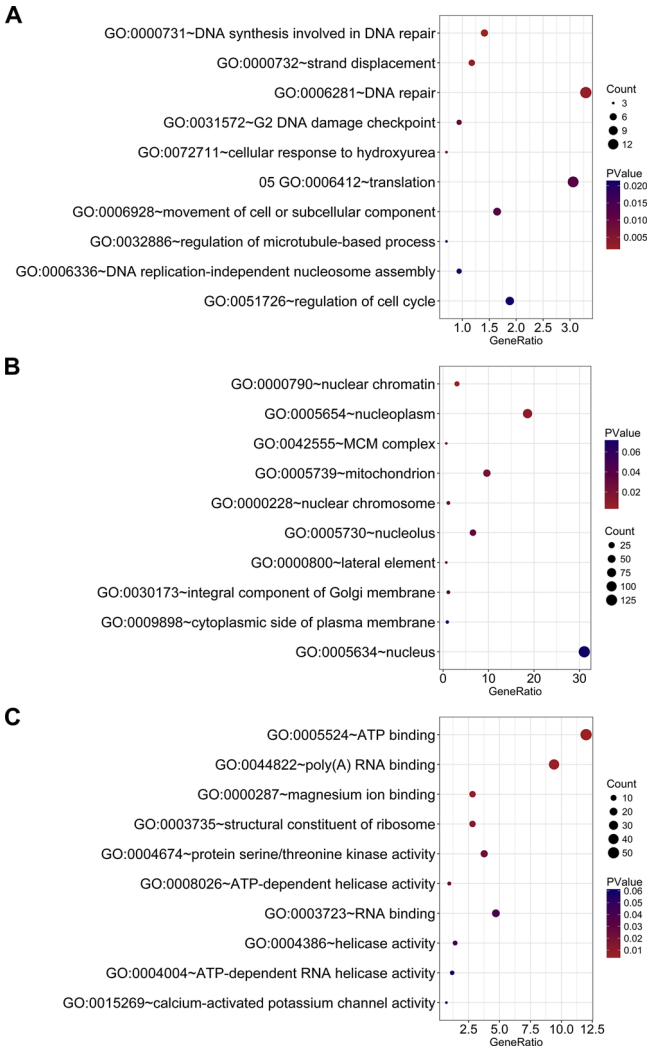

Fig. 9. Gene ontology (GO) analysis of the potential miR-449c-5p targets in the hepatocellular carcinoma (HCC) tissue samples. A: Biological process (BP) indicates that "DNA synthesis involved in DNA repair" is the most significant term; B: "Nuclear chromatin" ranks as the most marked category in cellular component (CC); C: Molecular function (MF) term suggests that "ATP binding" was enriched by targets of miR-449c-5p most significantly.

identification of 428 potential miR-449c-5p target genes that were then processed for pathway analysis (Fig. 7).

3.2.3. *The miR-449c-5p signaling pathways*

Multiple bioinformatic assessments were performed to evaluate the possible signaling pathways related to miR-449c-5p expression in HCC. The hub genes and the PPI network are shown in Fig. 8. GO analysis showed that the top terms for each annotation were DNA synthesis involved in DNA repair (BP), nuclear chromatin (CC), and ATP binding (MF) (Fig. 9). The KEGG analysis revealed four significant pathways (Fig. 10), with the top one being the pathway of homologous recombination that included four genes: *DNA polymerase delta 3* (*POLD3*), *RAD51 paralog C* (*RAD51C*), *BLM RecQ like helicase* (*BLM*) and *RAD51 recombinase* (*RAD51*, Table 2). The potential target gene *POLD3* was selected for verification using mRNA and protein expression data. In the Oncomine database, a search for "POLD3" for the gene, "Cancer vs. Normal Analysis" for the analysis type and "liver cancer" for the cancer type identified eight differential analyses. Among these eight studies, six studies found that *POLD3* expression levels followed a decreasing trend in HCC tissues compared to non-cancerous liver controls. The six studies included the Guichard Liver (Fig. 11), the Guichard Liver 2 (Fig. 12), the Wurmbach Liver (Fig. 13), the TCGA Liver (Fig. 14), the Mas Liver (Fig. 15) and the Chen Liver (Fig. 16).

From the immunohistochemical staining provided by Protein Atlas, 60% of the HCC samples presented negative POLD3 protein expression levels, and 100% of the normal liver sample showed weak expression (Fig. 17). In contrast to the miR-449c-5p expression levels, the POLD3 protein expression levels may be weaker in HCC tissues compared to non-cancerous liver tissues. However, since the sample number was too small for statistical analysis, the POLD3 protein levels and their relationship with miR-449c-5p in HCC should be validated in a larger cohort.

4. Discussion

In the current study, the overexpression of miR-449c-5p in HCC tissues was observed based on 238 HCC and 48 non-tumor tissue samples. The potential targets and relevant pathways of miR-449c-5p in HCC were further revealed through bioinformatics. These findings demonstrate that miR-449c-5p could play a crucial role in HCC by influencing diverse signaling pathways. Among the possible target genes, *POLD3* could be selected for future validation.

Little is known about the disease-related functions of miR-449c-5p, as evidenced by the few publications that were identified in our Pubmed search. Previous studies have explored the function of miR-449c-5p in CAVD pathogenesis. MiR-449c-5p has been shown to have a suppressive effect on the osteogenic differentiation of valve interstitial cells, which are responsible for calcific nodule formation in CAVD. Thus, miR-449c-5p may be a prospective target for treating CAVD [9]. Several reports have focused on the role and function of miR-449c-5p in neoplasms. Concordant downregulation of miR-449c-5p has been documented in osteosarcoma [10], non-small cell lung cancer [11], nasopharyngeal carcinoma [12] and gastric carcinoma [13]. However, this is the first study to find an increasing trend of miR-449c-5p levels in HCC tissues compared to non-HCC liver tissues. Our study was based on two meta-analyses that calculated SMD (0.44 > 0) and sROC (0.68 > 0.6). An observed SMD > 0 demonstrated that miR-449c-5p had a higher expression level in HCC than that in non-tumor tissues, and statistical significance could be considered if the 95% CI did not

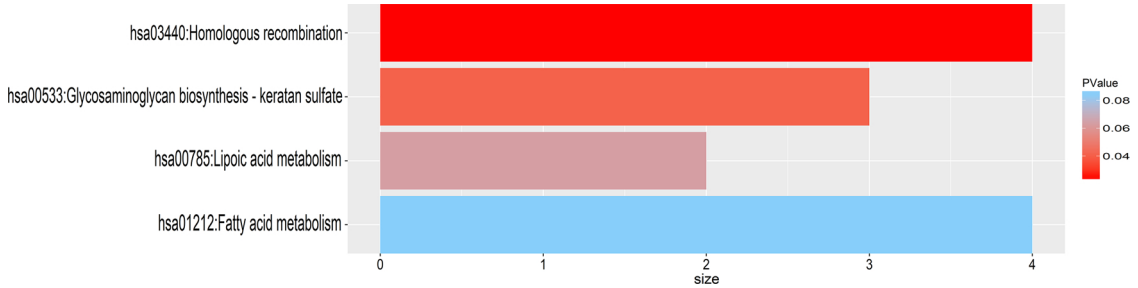

Fig. 10. Kyoto Encyclopedia of Genes and Genomes (KEGG) analysis of the potential miR-449c-5p targets in the hepatocellular carcinoma (HCC) tissue samples. Four pathways were identified with a P value < 0.05.

Table 2
The signaling pathways related to miR-449c-5p expression in hepatocellular carcinoma (HCC) tissue samples.

Category	Term	Count	P Value	Genes	FDR
GOTERM_BP_DIRECT	GO:0000731 ~ DNA synthesis involved in DNA repair	6	0.001023	POLD3, RAD51C, BLM, BRCA1, RAD51, RBBP8	1.701357
GOTERM_BP_DIRECT	GO:0000732 ~ strand displacement	5	0.002504	RAD51C, BLM, BRCA1, RAD51, RBBP8	4.114049
GOTERM_BP_DIRECT	GO:0006281 ~ DNA repair	14	0.002525	RAD51C, CLSPN, APEX2, USP3, BLM, PDS5A, etc.	4.148862
GOTERM_BP_DIRECT	GO:0031572 ~ G2 DNA damage checkpoint	4	0.009568	CLSPN, CDC14B, BRCA1, RBBP8	14.8798
GOTERM_BP_DIRECT	GO:0072711 ~ cellular response to hydroxyurea	3	0.009747	BLM, DDX11, RAD51	15.13812
GOTERM_BP_DIRECT	GO:0006412 ~ translation	13	0.011916	MRPL42, SLC25A6, RPL22L1, MRRF, RPS4X, RPL28, SLC25A13, etc.	18.1992
GOTERM_BP_DIRECT	GO:0006928 ~ movement of cell or subcellular components	7	0.012688	CXCR5, LTB4R, CAPZA2, ABI3, FPR3, CHST4, etc.	19.2633
GOTERM_BP_DIRECT	GO:0032886 ~ regulation of microtubule-based processes	3	0.016222	MACF1, DIAPH1, CLASP2	23.97256
GOTERM_BP_DIRECT	GO:0006336 ~ DNA replication-independent nucleosome assembly	4	0.019773	HIST1H4A, NASP, HIRA, HIST1H4D	28.44198
GOTERM_BP_DIRECT	GO:0051726 ~ regulation of cell cycle	8	0.021586	CDK19, NUP214, YY1AP1, FIGNL1, MADD, BOP1, etc.	30.62789
GOTERM_CC_DIRECT	GO:0000790 ~ nuclear chromatin	13	0.001062	PCGF2, DDX11, HDAC1, USP3, HIST1H1A, CREB1, etc.	1.442092
GOTERM_CC_DIRECT	GO:0005654 ~ nucleoplasm	79	0.009244	RAD51C, CLSPN, RAI1, CDC14B, RBM3, HIRA, etc.	11.92806
GOTERM_CC_DIRECT	GO:0042555 ~ MCM complex	3	0.015253	MCM7, MMS22 L, MCM3	18.95886
GOTERM_CC_DIRECT	GO:0005739 ~ mitochondrion	41	0.022328	RAD51C, RAI1, MRPL42, YWHAZ, SLC9A6, APEX2, etc.	26.57006
GOTERM_CC_DIRECT	GO:0000228 ~ nuclear chromosome	5	0.027665	HIST1H4A, BLM, FIGNL1, HIST1H4D, RAD51	31.86658
GOTERM_CC_DIRECT	GO:0005730 ~ nucleolus	28	0.033653	ING3, APEX2, BLM, CDC14B, RBM3, NUFIP1, etc.	37.38658
GOTERM_CC_DIRECT	GO:0000800 ~ lateral element	3	0.035904	BLM, BRCA1, RAD51	39.35235
GOTERM_CC_DIRECT	GO:0030173 ~ integral component of the Golgi membrane	5	0.036883	ST3GAL3, SLC35B4, ENTPD4, STEAP2, TBC1D20	40.18894
GOTERM_CC_DIRECT	GO:0009898 ~ cytoplasmic side of the plasma membrane	4	0.062353	ATP2B1, GM2A, IKBKB, RNF31	58.54418
GOTERM_CC_DIRECT	GO:0005634 ~ nucleus	132	0.072952	RAD51C, ALAD, CTDSPL, RBM3, STK36, HIRA, etc.	64.51337
GOTERM_MF_DIRECT	GO:0005524 ~ ATP binding	51	0.00271	CDK19, ADCY3, RAD51C, VARS2, FIGNL1, STK36, etc.	3.882269
GOTERM_MF_DIRECT	GO:0044822 ~ poly(A) RNA binding	40	0.004673	MRPL42, YWHAZ, DIAPH1, RBM3, ZNF638, BOP1, etc.	6.605529
GOTERM_MF_DIRECT	GO:0000287 ~ magnesium ion binding	12	0.006389	THTPA, RPS6KA4, SNRK, FIGNL1, STK36, PI4K2A, etc.	8.926892
GOTERM_MF_DIRECT	GO:0003735 ~ structural constituent of the ribosome	12	0.011656	MRPL42, SLC25A13, SLC25A24, SLC25A6, RPL21, SLC25A27, etc.	15.72213
GOTERM_MF_DIRECT	GO:0004674 ~ protein serine/threonine kinase activity	16	0.022942	PRKCA, CDK19, LIMK1, STK36, AURKC, PAK6, etc.	28.72399
GOTERM_MF_DIRECT	GO:0008026 ~ ATP-dependent helicase activity	4	0.026461	BLM, DDX11, DHX29, DHX33	32.37894
GOTERM_MF_DIRECT	GO:0003723 ~ RNA binding	20	0.040188	ADAD2, SETD1B, RBM3, NXF2, NUFIP1, ZNF638, etc.	45.0331
GOTERM_MF_DIRECT	GO:0004386 ~ helicase activity	6	0.041996	BLM, DDX11, DHX37, DHX34, DHX33, DDX10	46.52449
GOTERM_MF_DIRECT	GO:0004004 ~ ATP-dependent RNA helicase activity	5	0.057721	DHX29, DHX37, DHX34, DHX33, DDX10	57.9962
GOTERM_MF_DIRECT	GO:0015269 ~ calcium-activated potassium channel activity	3	0.06043	KCNN1, MTMR6, KCNMB1	59.72404
KEGG_PATHWAY	hsa03440: Homologous recombination	4	0.024247	POLD3, RAD51C, BLM, RAD51	26.78479
KEGG_PATHWAY	hsa00533: Glycosaminoglycan biosynthesis - keratan sulfate	3	0.040851	ST3GAL3, B4GALT3, CHST4	41.12488
KEGG_PATHWAY	hsa00785: Lipoic acid metabolism	2	0.063729	LIAS, LIPT1	56.67224
KEGG_PATHWAY	hsa01212: Fatty acid metabolism	4	0.085498	ACAA2, CPT1B, FADS1, SCD	67.86388

If there were more than six genes in the annotation/pathway, only the first six genes were listed in the table. FRD: False Discovery Rate.

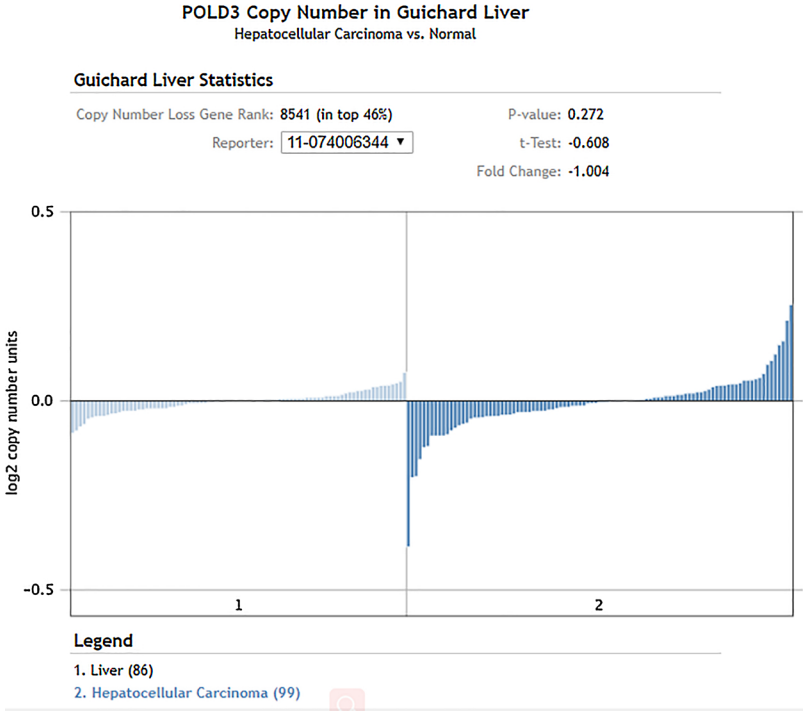

Fig. 11. The POLD3 expression levels in the hepatocellular carcinoma (HCC) tissues and the non-cancerous liver controls in the Guichard Liver microarray. In the Guichard Liver microarray, the expression levels of 18,823 genes were measured from 185 samples using the RefSeq Genes platform (UCSC refGene, July 2009, hg18, NCBI 36.1, March 2006).

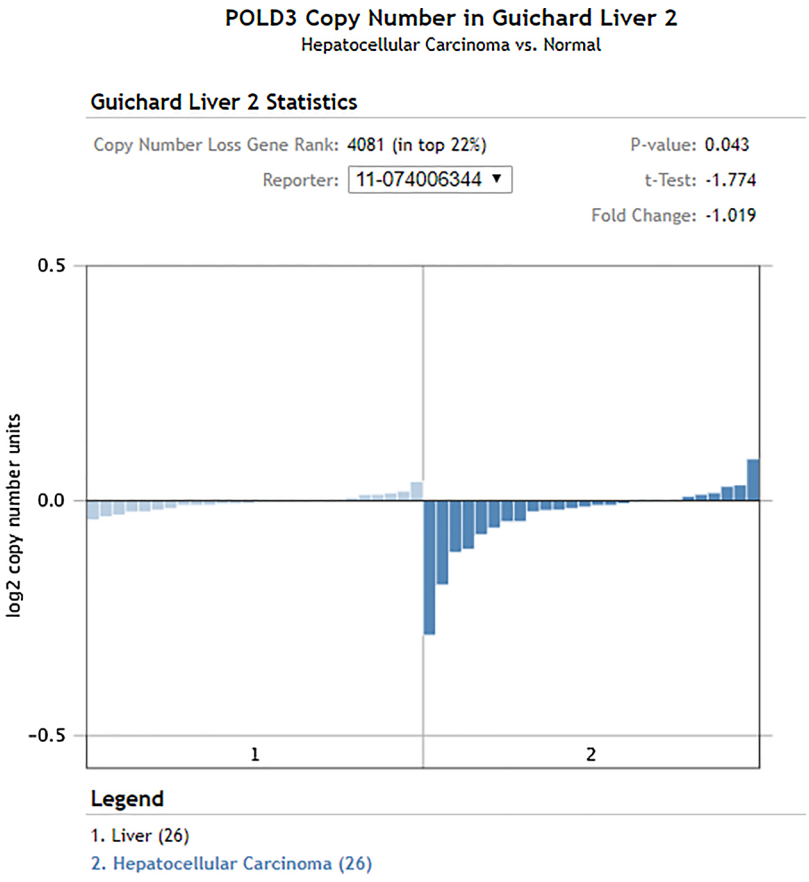

Fig. 12. The POLD3 expression levels in the hepatocellular carcinoma (HCC) tissues and the non-cancerous liver controls in the Guichard Liver 2 microarray. In the Guichard Liver 2 microarray, the expression levels of 18,823 genes were measured from 52 samples using the RefSeq Genes platform (UCSC refGene, July 2009, hg18, NCBI 36.1, March 2006).

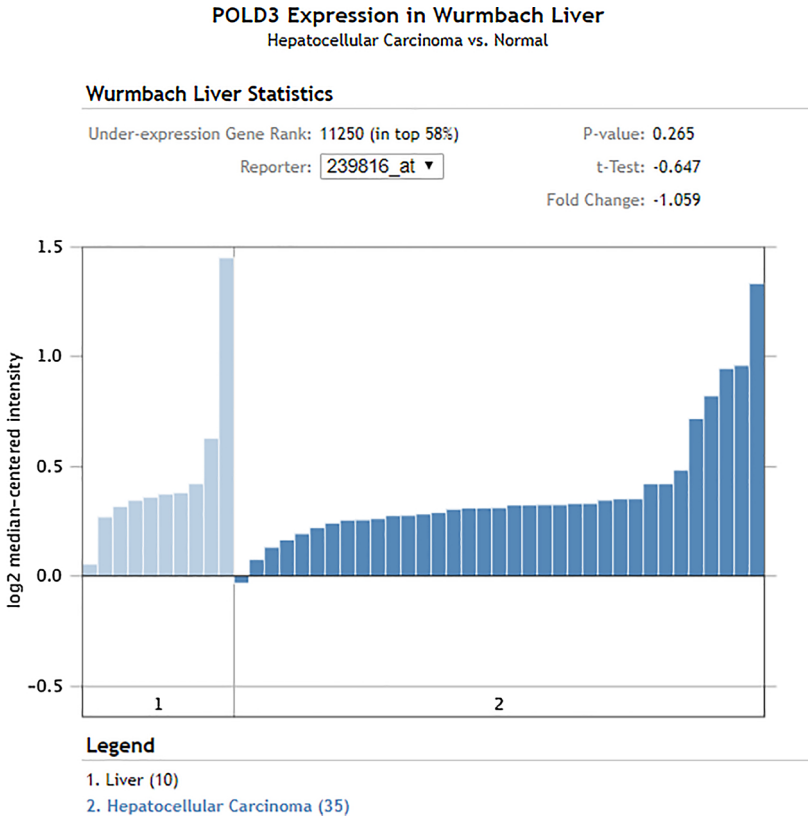

Fig. 13. The POLD3 expression levels in the hepatocellular carcinoma (HCC) tissues and the non-cancerous liver controls in the Wurmbach Liver microarray. In the Wurmbach Liver microarray, the expression levels of 19,574 genes were measured from 75 samples using the Human Genome U133 Plus 2.0 Array platform.

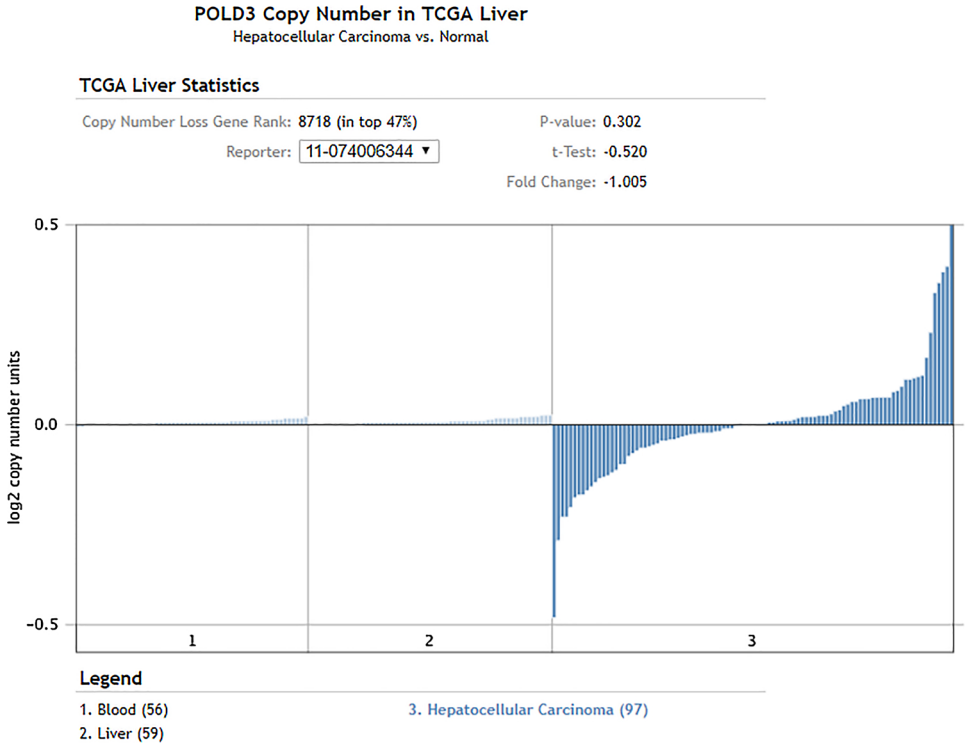

Fig. 14. The POLD3 expression levels in the hepatocellular carcinoma (HCC) tissues and the non-cancerous liver controls in the TCGA Liver microarray performed in 2012. In the TCGA Liver microarray, the expression levels of 18,823 genes were measured from 212 samples using the RefSeq Genes platform (UCSC refGene, July 2009, hg18, NCBI 36.1, March 2006).

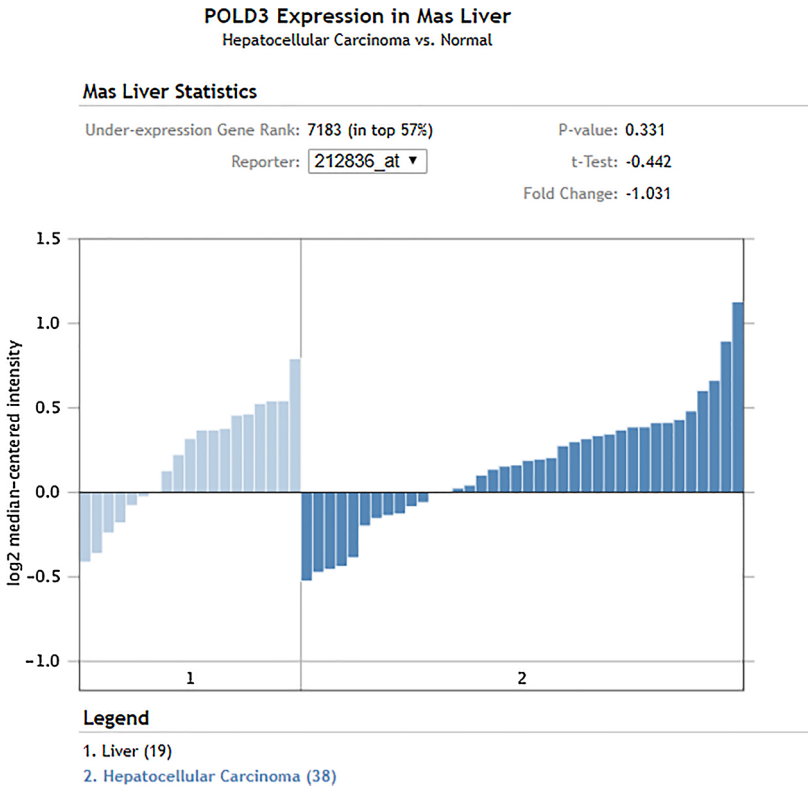

Fig. 15. The POLD3 expression levels in the hepatocellular carcinoma (HCC) tissues and the non-cancerous liver controls in the Mas Liver microarray. In the Mas Liver microarray, the expression levels of 12,603 genes were measured from 115 samples using the Human Genome U133 Plus 2.0 Array platform.

cross 0. Moreover, this was supported by a moderate AUC of 0.68 for miR-449c-5p. miR-449c-5p expression levels have also been implicated in osteosarcoma development, with miR-449c-5p expression shown to be inversely related to both tumor size and tumor Musculoskeletal Tumor Society (MSTS) Staging System [10]. A similar role has been confirmed in gastric carcinoma, where downregulated miR-449c-5p levels have been correlated to poorer survival [13,14]. But, the relationship between miR-449c-5p expression levels and HCC development has not been previously examined. Based on our limited HCC sample size that included both miR-449c-5p expression levels and survival information, we failed to observe a significant correlation between miR-449c-5p expression levels and patient outcome, even though

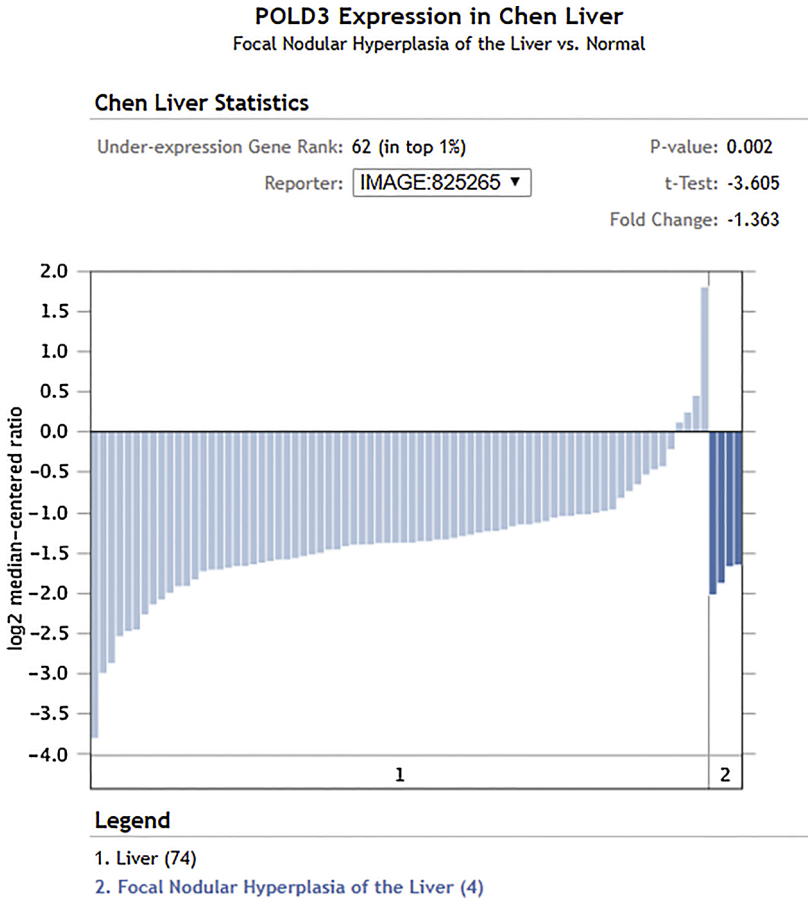

Fig. 16. The POLD3 expression levels in the hepatocellular carcinoma (HCC) tissues and the non-cancerous liver controls in the Chen Liver microarray. In the Chen Liver microarray, the expression levels of 10,802 genes were measured from 197 samples using the platform not pre-defined in Oncomine.

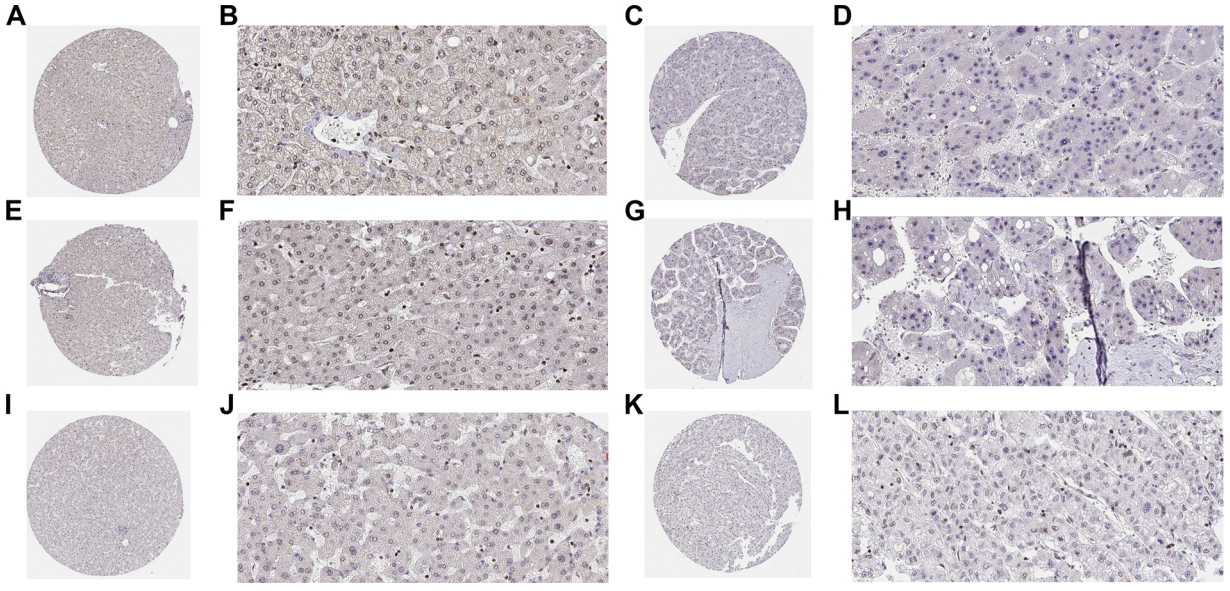

Fig. 17. The POLD3 protein expression levels in the hepatocellular carcinoma (HCC) tissues and the non-cancerous liver controls from Protein Atlas. A, B, E, F, I and J are non-cancerous liver tissues with moderate staining of POLD3. C, D, G, H, K and L are HCC tissues with negative staining of POLD3 (immunohistochemistry). The samples in the round shape: x 40; the samples in the square shape: x 400.

the HR was 1.25. The clinical role of miR-449c-5p in HCC may vary from that of other cancers, possibly due to variations in the target genes for each disease.

So far, only a few of the potential miR-449c-5p target genes have been verified: *6-phosphofructo-2-kinase* [14], *MET* [13], *c-MYC* [10,11], *SMAD4* [9] and *SOX4* [15]. In the current study, the potential miR-449c-5p target genes in HCC were defined using two independent methods. First, 2244 downregulated genes were identified after a miR-

449c-5p mimic was transfected into an HCC cell line. These down-regulated genes were considered to be influenced by miR-449c-5p in HCC cells. Since these DEGs could be either direct miR-449c-5p target genes or indirectly affected genes, we overlapped this gene pool with 5217 candidate miR-449c-5p target genes predicted by online software. The final 428 genes thus had a higher probability to act as actual miR-449c-5p targets in HCC. These 428 potential miR-449c-5p target genes were primarily enriched in the pathway of homologous recombination. Homologous recombination-mediated DNA repair has been shown to play a pivotal role in several malignancies [44–46]. One gene in the homologous recombination pathway that attracted our interest was *POLD3*, as it has not been previously investigated in HCC. POLD3 is an accessory subunit of the replicative Pol δ polymerase, which plays a significant role in DNA repair and translation synthesis through the polymerase Pol ζ. Previous studies have shown that POLD3 depletion leads to increased genomic instability (as manifested by DNA breaks, S-phase progression impairment and chromosome abnormalities [47]) which is crucial for cellular proliferation. Interestingly, not many studies have focused on the role and function of POLD3 in cancers. We found that POLD3 mRNA and protein expression levels showed a decreasing trend in HCC tissues, as detected by microarray/RNA-sequence and immunohistochemistry. There is a significant possibility that POLD3 is an actual miR-449c-5p target in HCC due to the following three factors: 1) *POLD3* was profoundly downregulated when HCC cells were transfected with miR-449c-5p in vitro; 2) *POLD3* was predicted by miRWalk to be a prospective miR-449c-5p target with a high score of 1; and 3) there was a decreasing trend in POLD3 expression in HCC tissues, directly opposite to that of miR-449c-5p. However, these bioinformatic findings should be validated with further experiments.

Since the upregulation of miR-449c-5p could play an integral role in HCC tumorigenesis, treatments that inhibit its expression could have therapeutic potential. The green tea polyphenol epigallocatechin-3-gallate (EGCG) is an example of a potential therapeutic candidate. Previous reports have demonstrated that EGCG suppresses malignancies through its antioxidant activity and that miR-449c-5p is involved in the molecular mechanism of EGCG treatment [48].

Due to the limitations of the current work, further validations should be carried out: 1) The clinical role of miR-449c-5p should be explored in a larger sample size; 2) Similar validation should be conducted to confirm that POLD3 is downregulated or absent in HCC clinical tissues; and 3) A dual luciferase reporter assay should be used to validate this targeting relationship. In vitro and in vivo experiments should also be performed to study the function of miR-449c-5p and POLD3 in HCC.

In summary, the current findings suggest that miR-449c-5p upregulation could play an essential role in HCC through various pathways. Whether miR-449c-5p exerts its function by targeting POLD3 should be explored in future experiments.

Declaration of interest

The authors declare no conflict of interest.

Funding source statements

This study was supported by the Education Innovation Fund designated for graduate students of Guangxi Province (Grant No. YCBZ2015026) and the Foundation for the Promotion of the Basic Ability of Young and Middle-aged Teachers in the Universities of Guangxi (Grant No. 2018KY0120)

References

[1] M. Reig, L.G. da Fonseca, S. Faivre, New trials and results in systemic treatment of HCC, J. Hepatol. 69 (2018) 525–533.
[2] P. Vande Lune, A.K. Abdel Aal, S. Klimkowski, J.G. Zarzour, A.J. Gunn, Hepatocellular carcinoma: Diagnosis, treatment algorithms, and imaging appearance after transarterial chemoembolization, J. Clin. Transl. Hepatol. 6 (2018) 175–188.
[3] Y. Zhang, Y.W. Dang, X. Wang, et al., Comprehensive analysis of long non-coding RNA PVT1 gene interaction regulatory network in hepatocellular carcinoma using gene microarray and bioinformatics, Am. J. Transl. Res. 9 (2017) 3904–3917.
[4] H. Yang, X. Zhang, X.Y. Cai, et al., From big data to diagnosis and prognosis: gene expression signatures in liver hepatocellular carcinoma, Peer J. 5 (2017) e3089.
[5] R. He, L. Gao, J. Ma, et al., The essential role of MTDH in the progression of HCC: a study with immunohistochemistry, TCGA, meta-analysis and in vitro investigation, Am. J. Transl. Res. 9 (2017) 1561–1579.
[6] F. Vasuri, M. Visani, G. Acquaviva, et al., Role of microRNAs in the main molecular pathways of hepatocellular carcinoma, World J. Gastroenterol. 24 (2018) 2647–2660.
[7] C.Y. Li, Y.Y. Pang, H. Yang, et al., Identification of miR-101-3p targets and functional features based on bioinformatics, meta-analysis and experimental verification in hepatocellular carcinoma, Am. J. Transl. Res. 9 (2017) 2088–2105.
[8] L. Liang, J.H. Zeng, J.Y. Wang, et al., Down-regulation of miR-26a-5p in hepatocellular carcinoma: A qRT-PCR and bioinformatics study, Pathol. Res. Pract. 213 (2017) 1494–1509.
[9] R. Xu, M. Zhao, Y. Yang, et al., MicroRNA-449c-5p inhibits osteogenic differentiation of human VICs through Smad4-mediated pathway, Sci. Rep. 7 (2017) 8740.
[10] Q. Li, H. Li, X. Zhao, et al., DNA methylation mediated downregulation of miR-449c controls osteosarcoma cell cycle progression by directly targeting oncogene c-Myc, Int. J. Biol. Sci. 13 (2017) 1038–1050.
[11] L.J. Miao, S.F. Huang, Z.T. Sun, et al., MiR-449c targets c-Myc and inhibits NSCLC cell progression, FEBS Lett. 587 (2013) 1359–1365.
[12] F. Wang, J. Lu, X. Peng, et al., Integrated analysis of microRNA regulatory network in nasopharyngeal carcinoma with deep sequencing, J. Exp. Clin. Cancer Res. 35 (2016) 17.
[13] Z. Wu, H. Wang, S. Fang, C. Xu, MiR-449c inhibits gastric carcinoma growth, Life Sci. 137 (2015) 14–19.
[14] X. Chen, A. Wang, X. Yue, miR-449c inhibits migration and invasion of gastric cancer cells by targeting PFKFB3, Oncol. Lett. 16 (2018) 417–424.
[15] M. Sandbothe, R. Buurman, N. Reich, et al., The microRNA-449 family inhibits TGF-beta-mediated liver cancer cell migration by targeting SOX4, J. Hepatol. 66 (2017) 1012–1021.
[16] D.Y. Wen, P. Lin, H.W. Liang, et al., Up-regulation of CTD-2547G23.4 in hepatocellular carcinoma tissues and its prospective molecular regulatory mechanism: A novel qRT-PCR and bioinformatics analysis study, Cancer Cell Int. 18 (2018) 74.
[17] Y.P. Chow, H. Alias, R. Jamal, Meta-analysis of gene expression in relapsed childhood B-acute lymphoblastic leukemia, BMC Cancer 17 (2017) 120.
[18] Y. Zhang, J.C. Huang, K.T. Cai, et al., Long noncoding RNA HOTTIP promotes hepatocellular carcinoma tumorigenesis and development: A comprehensive investigation based on bioinformatics, qRTPCR and metaanalysis of 393 cases, Int. J. Oncol. 51 (2017) 1705–1721.
[19] X. Gao, R.X. Tang, Q.N. Xie, et al., The clinical value of miR-193a-3p in non-small cell lung cancer and its potential molecular mechanism explored in silico using RNA-sequencing and microarray data, FEBS Open Bio 8 (2018) 94–109.
[20] Z.C. Xie, Y.W. Dang, D.M. Wei, et al., Clinical significance and prospective molecular mechanism of MALAT1 in pancreatic cancer exploration: A comprehensive study based on the GeneChip, GEO, Oncomine, and TCGA databases, Onco. Ther. 10 (2017) 3991–4005.
[21] Q.L. Huang, F.J. Zhou, C.B. Wu, et al., Circulating biomarkers for predicting infliximab response in rheumatoid arthritis: a systematic bioinformatics analysis, Med. Sci. Monit. 23 (2017) 1849–1855.
[22] H. Ding, Z.H. Ye, D.Y. Wen, et al., Downregulation of miR1365p in hepatocellular carcinoma and its clinicopathological significance, Mol. Med. Rep. 16 (2017) 5393–5405.
[23] G.A. Kelley, K.S. Kelley, Exercise and cancer-related fatigue in adults: a systematic review of previous systematic reviews with meta-analyses, BMC Cancer 17 (2017) 693.
[24] M. Zhang, H. Ma, J. Zhang, L. He, X. Ye, X. Li, Comparison of microwave ablation and hepatic resection for hepatocellular carcinoma: a meta-analysis, Onco Targets Ther. 10 (2017) 4829–4839.
[25] R. Zhang, B. Chen, X. Tong, et al., Diagnostic accuracy of droplet digital PCR for detection of EGFR T790M mutation in circulating tumor DNA, Cancer Manag. Res. 10 (2018) 1209–1218.
[26] H.B. Yan, J.C. Huang, Y.R. Chen, et al., Role of miR-1 expression in clear cell renal cell carcinoma (ccRCC): A bioinformatics study based on GEO, ArrayExpress microarrays and TCGA database, Pathol. Res. Pract. 214 (2018) 195–206.
[27] H.B. Shi, J.X. Yu, J.X. Yu, et al., Diagnostic significance of microRNAs as novel biomarkers for bladder cancer: a meta-analysis of ten articles, World J. Surg. Oncol. 15 (2017) 147.
[28] R. Aguirre-Gamboa, V. Trevino, SurvMicro: Assessment of miRNA-based prognostic signatures for cancer clinical outcomes by multivariate survival analysis, Bioinformatics 30 (2014) 1630–1632.
[29] F. Zou, J. Li, X. Jie, et al., Rs3842530 polymorphism in microRNA-205 host gene in lung and breast cancer patients, Med. Sci. Monit. 22 (2016) 4555–5464.
[30] H. Dweep, N. Gretz, C. Sticht, miRWalk database for miRNA-target interactions, Methods Mol. Biol. 1182 (2014) 289–305.
[31] S. Chen, X. Qi, H. Chen, et al., Expression of miRNA-26a in platelets is associated with clopidogrel resistance following coronary stenting, Exp. Ther. Med. 12 (2016) 518–524.
[32] J.Y. Liu, J.B. Lu, Y. Xu, MicroRNA-153 inhibits the proliferation and invasion of

human laryngeal squamous cell carcinoma by targeting KLF5, Exp. Ther. Med. 11 (2016) 2503–2508.
[33] C.Z. Liu, Z.H. Ye, J. Ma, et al., A qRT-PCR and gene functional enrichment study focused on downregulation of miR-141-3p in hepatocellular carcinoma and its clinicopathological significance, Technol. Cancer Res. Treat. 16 (2017) 835–849.
[34] H.W. Liang, Z.H. Ye, S.Y. Yin, et al., A comprehensive insight into the clinicopathologic significance of miR-144-3p in hepatocellular carcinoma, Onco Targets Ther. 10 (2017) 3405–3419.
[35] X. Zhang, Z.H. Ye, H.W. Liang, et al., Down-regulation of miR-146a-5p and its potential targets in hepatocellular carcinoma validated by a TCGA- and GEO-based study, FEBS Open Biol. 7 (2017) 504–521.
[36] X. Yang, Y.Y. Pang, R.Q. He, et al., Diagnostic value of strand-specific miRNA-101-3p and miRNA-101-5p for hepatocellular carcinoma and a bioinformatic analysis of their possible mechanism of action, FEBS Open Biol. 8 (2018) 64–84.
[37] C. Qian, Y. Xia, Y. Ren, Y. Yin, A. Deng, Identification and validation of PSAT1 as a potential prognostic factor for predicting clinical outcomes in patients with colorectal carcinoma, Oncol. Lett. 14 (2017) 8014–8020.
[38] J. Meng, L.H. Wang, C.L. Zou, S.M. Dai, J. Zhang, Y. Lu, C10orf116 gene copy number loss in prostate cancer: Clinicopathological correlations and prognostic significance, Med. Sci. Monit. 23 (2017) 5176–5183.
[39] R. Peng, X. Huang, C. Zhang, X. Yang, Y. Xu, D. Bai, Overexpression of UHRF2 in intrahepatic cholangiocarcinoma and its clinical significance, Onco Targets Ther. 10 (2017) 5863–5872.
[40] P.J. Thul, C. Lindskog, The human protein atlas: a spatial map of the human proteome, Protein Sci. 27 (2018) 233–244.
[41] M. Uhlen, C. Zhang, S. Lee, et al., A pathology atlas of the human cancer transcriptome, Science 357 (2017), https://doi.org/10.1126/science.aan2507 eaan2507.
[42] E.H. Panosyan, H.J. Lin, J. Koster, J.L. Lasky, In search of druggable targets for GBM amino acid metabolism, BMC Cancer 17 (2017) 162.
[43] R.Q. He, X.J. Li, L. Liang, et al., The suppressive role of miR-542-5p in NSCLC: the evidence from clinical data and in vivo validation using a chick chorioallantoic membrane model, BMC Cancer 17 (2017) 655.
[44] M. Cai, H. Zhang, L. Hou, et al., Inhibiting homologous recombination decreases extrachromosomal amplification but has no effect on intrachromosomal amplification in methotrexate-resistant colon cancer cells, Int. J. Cancer (2018), https://doi.org/10.1002/ijc.31781 [Epub ahead of print].
[45] D. Kim, Y. Liu, S. Oberly, R. Freire, M.B. Smolka, ATR-mediated proteome remodeling is a major determinant of homologous recombination capacity in cancer cells, Nucleic Acids Res. (2018), https://doi.org/10.1093/nar/gky625 [Epub ahead of print].
[46] Z. Sztupinszki, M. Diossy, M. Krzystanek, et al., Migrating the SNP array-based homologous recombination deficiency measures to next generation sequencing data of breast cancer, NPJ Breast Cancer 4 (2018) 16.
[47] E. Tumini, S. Barroso, C.P. Calero, A. Aguilera, Roles of human POLD1 and POLD3 in genome stability, Sci. Rep. 6 (2016) 38873.
[48] H. Zhou, J. Manthey, E. Lioutikova, et al., The up-regulation of Myb may help mediate EGCG inhibition effect on mouse lung adenocarcinoma, Hum. Genomics 10 (Suppl 2) (2016) 19.